Networks and Heterogeneous Media

https://www.aimspress.com/journal/nhm

NHM, 21(4): 1544–1579.
DOI: 10.3934/nhm.2026059
Received: 17 March 2026
Revised: 30 June 2026
Accepted: 10 July 2026
Published: 20 July 2026

Research article

Complex networks for the analysis and simulation of intermunicipal public transportation: A case study of the Department of Quindío, Colombia

Jorge Mario Garcia-Usuga[1,*], **Monica Jhoana Mesa-Mazo**[1] **and Jhoana P. Romero-Leiton**[2]

[1] Licenciatura en Matemáticas, Universidad del Quindío, cra 15 calle 12 Norte, Armenia-Quindío, Colombia

[2] University of Puerto Rico at Mayagüez, Mayagüez PR 00682, USA

* **Correspondence:** Email: jmgarcia@uniquindio.edu.co; Tel: +573013890634.

Abstract: This paper presents an integrated methodological framework for analyzing the structure and operational performance of intercity public transportation systems by combining complex network theory with discrete event simulation. The road network is modeled as a directed multigraph, enabling the identification of critical nodes and corridors through centrality metrics and percolation analysis, while the simulation operates directly on the network's topology by incorporating travel speed variability, passengers' boarding and alighting times, and service frequencies. A case study of the intercity public transportation network of the Department of Quindío (Colombia) demonstrates the applicability of the methodology. The results show that network vulnerability is concentrated in a limited number of strategic corridors, with betweenness centrality providing the most effective criterion for identifying structurally critical nodes. Furthermore, although alternative routes exist, they do not necessarily guarantee operational resilience. The proposed framework provides a quantitative decision support tool for transportation planning and infrastructure management and, owing to its modular and scalable design, can be readily adapted to other intercity transportation systems.

Keywords: complex networks; directed multigraph; public transportation; discrete event simulation; queueing theory; network resilience; intercity mobility

1. Introduction

Vehicular congestion and mobility disruptions represent major challenges for contemporary transportation systems, generating significant economic, social, and environmental impacts worldwide. According to the *Global Traffic Scorecard 2024* published by INRIX [1], drivers in the most congested cities globally lost between 88 and 105 hours annually due to traffic congestion. Similar trends have been reported across Europe and Asia, where cities such as Dublin, London, Beijing, and Delhi have experienced substantial increases in travel times and mobility demand [2]. These patterns highlight the growing pressure on transportation infrastructure and the need for more efficient and resilient mobility planning strategies.

Within this global context, Latin America faces distinctive structural challenges. The region hosts the largest global deployment of bus rapid transit (BRT) systems, transporting more than 21 million passengers daily, which reflects a strong reliance on public transport as a primary mobility solution [3–5]. However, public transportation systems in the region are frequently constrained by financial limitations, service informality, operational inefficiencies, and limited infrastructure investment. In Colombia, these challenges are intensified by high transportation costs, informal services, and accessibility gaps affecting both urban and rural populations [6, 7].

These problems become particularly relevant in Andean territories, where mountainous terrain and high exposure to extreme climatic events associated with El Niño–Southern Oscillation (ENSO) phenomena frequently disrupt strategic road corridors [8]. In countries such as Colombia, Peru, and Ecuador, landslides and road infrastructure failures generate significant economic losses and may isolate rural communities for prolonged periods, increasing territorial disparities in access to essential services [9, 10]. Under these conditions, intermunicipal public transportation systems are highly vulnerable, since their operation depends on road networks exposed to closures, deterioration, and limited redundancy.

From a methodological perspective, the analysis of transportation systems requires tools capable of evaluating both the structural properties of road networks and their operational performance. Complex network theory has emerged as a powerful framework for representing transportation infrastructures as graphs, where nodes and edges allow the identification of critical structural elements through centrality metrics, robustness measures, and percolation analysis [11–13]. Recent studies have shown that graph-based approaches are useful for evaluating resilience, vulnerability, and recovery strategies in public transport and interdependent transportation networks [14–17]. These works emphasize that failures affecting highly central or strategically located elements may produce disproportionate impacts on system connectivity and service performance.

Simulation-based approaches have also played an important role in the analysis of transportation systems. Discrete event simulation provides a flexible framework for representing operational processes such as vehicle movements, passengers boarding and alighting, travel time variability, and service frequencies [18–20]. Recent applications have combined discrete event simulation with empirical data, GPS information, and geographic information systems to evaluate congestion management, freight operations, and route performance under realistic operating conditions [21, 22]. In addition, simulation methods have been widely used to assess transportation infrastructure resilience, disruption impacts, and operational recovery strategies [20, 23].

Building upon these simulation approaches, recent advances in queueing theory have considerably expanded the analytical capabilities for modeling stochastic transportation and service systems. Modern formulations incorporate correlated arrival processes, multi server architectures, batch arrivals, dynamic priority mechanisms, and resource-sharing strategies, providing rigorous mathematical tools for evaluating systems' performance under uncertainty [24–26]. These approaches have been successfully applied to logistics systems, warehouses, hospitals, communication networks, and other service-oriented infrastructures, offering valuable insights into congestion, resource allocation, and operational efficiency.

Although complex network analysis, discrete event simulation, and queueing-based models have been extensively applied in transportation and service systems, they are often used as independent approaches. Most existing studies focus either on the structural characterization of transportation networks or on the operational simulation of service dynamics, with relatively limited integration between both perspectives. Consequently, there remains a need for methodologies capable of linking structural network properties with operational performance under realistic disruption scenarios, particularly in intermunicipal transportation systems operating in geographically complex regions.

Motivated by this research gap, the present study proposes an integrated methodological framework that combines complex network analysis with discrete event simulation to evaluate the intermunicipal public transportation system of the Department of Quindío, Colombia. Unlike approaches that analyze network structure and operational dynamics separately, the proposed framework explicitly connects both dimensions by using the road network to identify critical nodes and corridors, determine feasible transportation routes, estimate travel distances, and evaluate operational impacts under disruption scenarios.

The methodology includes the construction of a directed multigraph from OpenStreetMap data [27, 28], the identification of critical nodes and corridors through multiple centrality measures, resilience assessment, and percolation analysis [29, 30], and the development of a discrete event simulation model that incorporates passenger boarding and alighting processes together with travel speed variability. The resulting framework provides quantitative evidence to support transportation planning, route design, and contingency management, while offering a scalable methodology that can be adapted to other intermunicipal public transportation systems with similar geographical and operational characteristics.

2. Materials and methods

2.1. Study area

The study area corresponds to the department of Quindío (Figure 1), located in the Andean region of Colombia, with an approximate area of 1845 km^2 and a population close to 550,000 inhabitants [31]. The territory is characterized by a predominantly mountainous topography, steep slopes, high drainage density, and significant susceptibility to landslides. These conditions strongly influence the operation and reliability of the intermunicipal public transportation system.

The departmental road network connects 12 municipalities, with the city of Armenia acting as the central node of the system. This network constitutes a strategic mobility corridor supporting key regional economic activities such as coffee production, tourism, and regional trade.

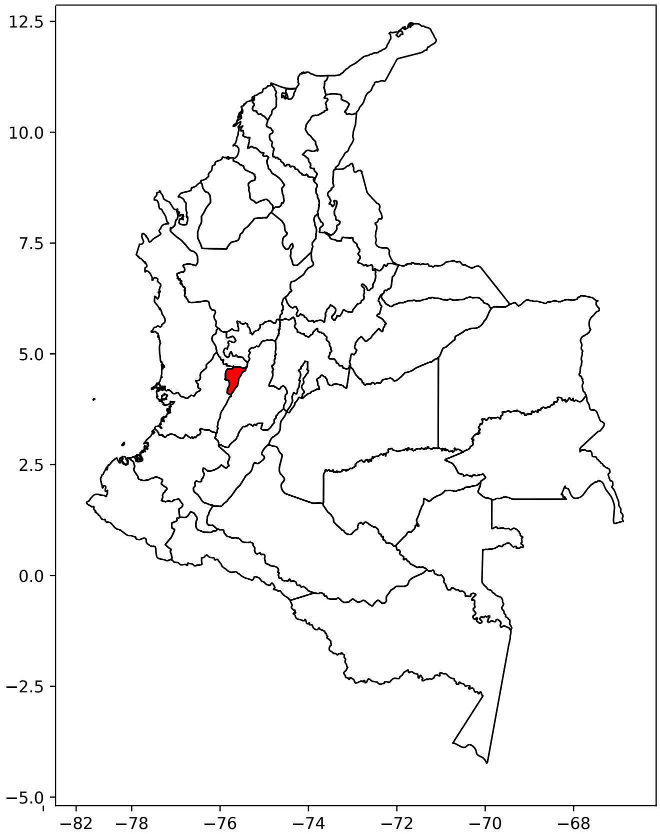

Figure 1. Location of the department of Quindío in Colombia.

2.2. Road network construction

The road network of the department of Quindío was constructed using open geospatial data obtained from OpenStreetMap (OSM) [32], using the `OSMnx` library [27, 28]. The network is represented as a directed graph $G = (V, E)$, specifically a multidigraph [33], where the set of nodes V represents road intersections, transportation terminals, and key municipal connection points, while the set of edges E represents road segments linking these nodes. Each edge is weighted according to its geographic length, as illustrated in Figure 2.

Within the network extracted using `OSMnx`, each node represents a road intersection or a relevant geometric transition point in the road infrastructure. Nodes store spatial and topological information including unique identifiers, geographic coordinates (latitude and longitude), and connectivity attributes derived from the network structure.

Edges represent road segments connecting nodes and include attributes describing their physical and operational characteristics, such as segment length, road type, number of lanes, directionality, geometric layout, and, when available, speed limits.

To facilitate storage, sharing, and the reproducibility of the constructed network, the graph was exported and stored in the `GraphML` format. This XML-based format preserves both the topological structure of the graph and the attributes associated with nodes and edges, including identifiers, lengths, directionality, and weights.

The constructed road network consists of 9141 nodes and 20,877 edges. The average node degree is 4.57, indicating that each node is connected to approximately 4.57 neighboring nodes on average. The calculated network density is 0.0002, which suggests a relatively sparse network structure typical of road transportation systems.

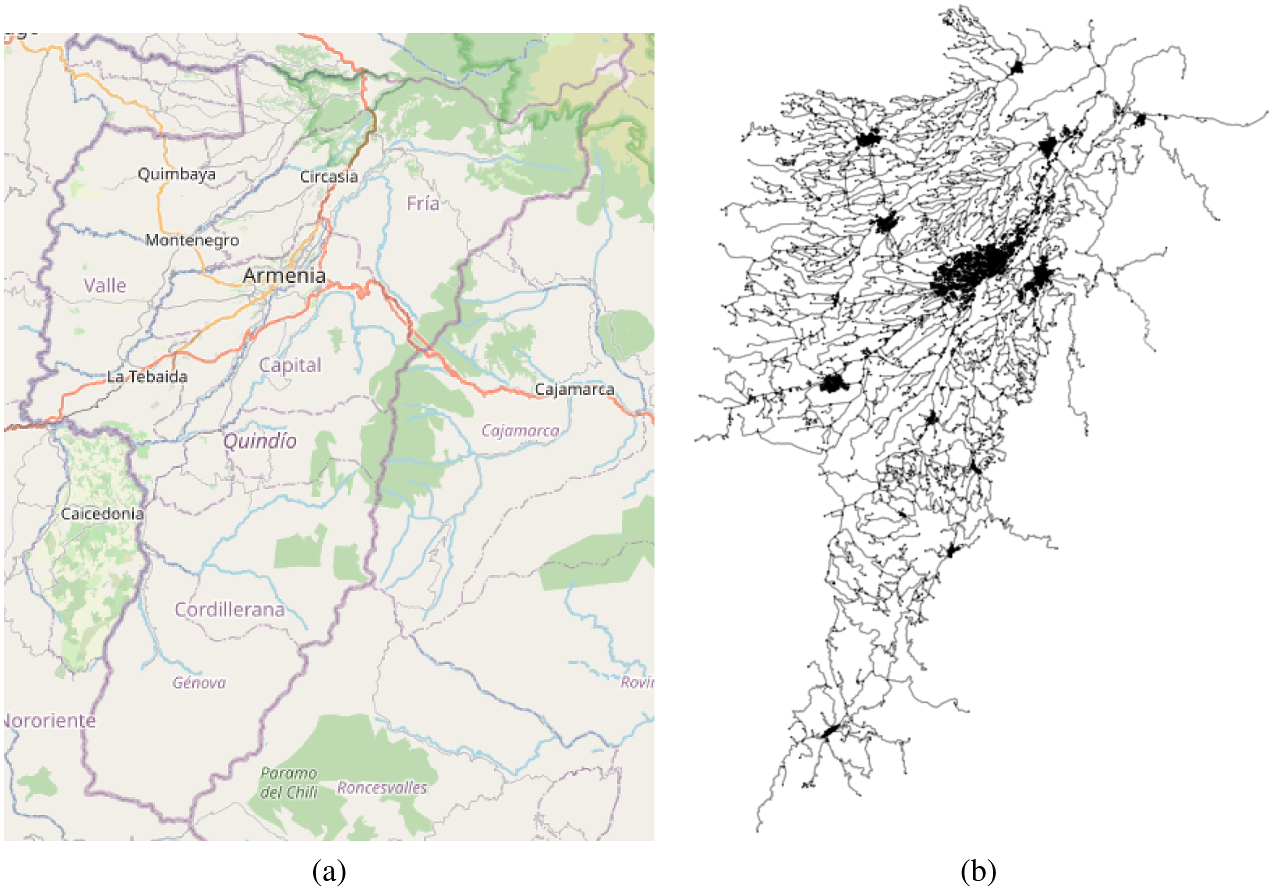

Figure 2. (a) Topographic map of the department of Quindío. (b) The corresponding road network extracted from `OpenStreetMap`.

2.3. *Centrality analysis and topological characterization*

A centrality analysis was performed on the constructed road network using tools from complex network theory [11–13, 34]. The following metrics were computed: Degree centrality, closeness centrality, betweenness centrality, eccentricity, eigenvector centrality, straightness centrality, and network resilience.

These metrics allow the identification of critical nodes and transportation corridors whose disruption could significantly affect the overall connectivity of the system. Additionally, the structural resilience of the network was evaluated through progressive removal scenarios targeting highly central nodes, analyzing the resulting network fragmentation and the loss of connectivity between municipalities [29, 30].

2.4. Resilience in complex networks

Resilience in complex networks refers to the ability of a system to resist, adapt to, and recover from internal or external perturbations while maintaining its essential functionality. In networked systems, this functionality is typically associated with global connectivity, the efficient transmission of information or resources, and the ability of nodes to remain interconnected.

According to Fraccascia et al. [35], the resilience of a complex system can be understood as its capacity to absorb disturbances, reorganize, and continue operating while preserving its structure and identity. This perspective highlights that resilience involves not only resistance to disruptions but also the adaptive capacity of the system under adverse dynamics.

From a structural perspective, Costa [36] defined network resilience as the robustness of the system against node removal, particularly when nodes are removed in a targeted manner according to their degree or centrality. This approach enables the evaluation of a network's vulnerability to intentional attacks and suggests reinforcement strategies through the addition of alternative links.

Similarly, Paul et al. [37] analyzed resilience by estimating the critical fraction of nodes, denoted as f_c, whose random removal leads to the loss of global connectivity. This methodology relies on Monte Carlo simulations and allows the estimation of structural tolerance thresholds for different network topologies such as scale-free or bimodal networks.

Furthermore, Gao et al. [38] proposed a general analytical framework for complex dynamic systems in which resilience is characterized as a transition from a functional to a non functional state under parameter variations. Their approach introduces the macroscopic parameter β_{eff}, which summarizes the combined effects of multiple structural and dynamical perturbations and allows the system's dynamics to be described through a universal resilience function.

In infrastructure networks such as road systems, resilience is typically evaluated by analyzing changes in network connectivity after removing nodes that represent intersections or road segments. These analyses include simulations of targeted attacks (based on the degree or centrality) and random failures, monitoring the evolution of the giant connected component and calculating indicators such as the area under the connectivity curve to estimate the overall resilience of the system.

2.5. Simulation of public transport on the Quindío road network

To model the dynamics of intermunicipal public transportation, a discrete event simulation was implemented using the `SimPy` library in Python [39]. The simulation operates on the previously constructed road network obtained by `OSMnx` [27, 28], represented as a weighted directed graph (Figure 2), where nodes correspond to road intersections and the edges correspond to road segments with attributes such as length and estimated travel time.

The simulation is inspired by concepts from queueing theory but does not assume a classical analytical queueing model such as an Markovian/Markovian/single-server (M/M/1) queueing model. Instead, it implements an event-driven discrete event simulation in which vehicle movements trigger the operational events occurring along the route. Passenger exchanges take place only when the bus reaches predefined stopping locations; consequently, passenger generation is associated with bus arrivals rather than with an independent temporal arrival process. The model therefore focuses on representing the operational behavior of intermunicipal public transport under realistic road conditions rather than on reproducing passenger demand dynamics.

Bus routes are predefined according to the operating schedules established by the transportation companies. Consequently, each simulated bus follows a fixed route without interacting with vehicles assigned to other routes, reflecting the actual operational organization of intermunicipal public transport in the department of Quindío. Likewise, transfers between routes are not considered. Traffic congestion is also not modeled explicitly because the analyzed routes are predominantly intermunicipal and operate on road corridors with a relatively low traffic density. Instead, local traffic conditions are incorporated indirectly through stochastic variations in the travel speed assigned to each road segment.

Passengers boarding and alighting are represented by bounded stochastic variables derived from field observations, while travel times depend on both the geometric characteristics of the road network and the operational variability introduced through speed fluctuations. Although passenger demand in rural transportation may exhibit seasonal or batch-arrival patterns, modeling demand generation is beyond the scope of the present work. The proposed framework focuses on evaluating the operational consequences of the road network's structure on travel times and route performance. Future extensions of the model may incorporate demand-driven passenger generation and sensitivity analyses with respect to different passenger arrival processes.

The complete road network was divided into zones representing key segments of the routes connecting selected municipalities with strategic nodes of the system, particularly the Armenia transportation terminal, located in the departmental capital. Each zone is defined by a starting node, an ending node, and a range of average speeds ($v_{\min}, v_{\max}$), which are randomly assigned during each simulation run. Additionally, each zone includes specific rules governing passenger boarding and alighting processes.

The interaction between the complex road network and the discrete event simulation occurs throughout the entire simulation process rather than only at its final stage. The graph extracted from OpenStreetMap provides the topological structure on which the simulation operates by determining the feasible routes between consecutive zones through shortest-path algorithms, supplying the geometric length of every road segment, and defining the sequence of nodes traversed by each vehicle. Consequently, the operational behavior simulated in `SimPy` is directly constrained by the underlying network topology, since travel times, route lengths, intermediate stopping locations, and alternative paths under disruption scenarios are all computed from the graph representation. This integration ensures that the discrete event simulation is network-driven rather than operating on an abstract representation of predefined travel times.

Within each zone segment, two intermediate nodes are randomly selected as bus stops. At these stops, passengers board or alight from the vehicle according to bounded random values constrained by the maximum bus capacity. The stochastic parameters used in the simulation are derived from empirical observations of real bus routes, including typical travel times and operating speeds.

The distance between consecutive nodes is obtained from the `length` attribute of the road graph, and the travel time between nodes is computed using the following relation:

$$t_{ij} = \frac{d_{ij}}{v} \cdot 60, \tag{2.1}$$

where d_{ij} represents the road length between nodes i and j expressed in kilometers, and v denotes the bus's speed in km/h. The resulting travel time is expressed in minutes to maintain consistency with the simulation time scale.

Each bus begins its route with a partial passenger load and sequentially traverses the predefined zones while accumulating the total travel time. The simulation records events such as passengers boarding, passengers alighting, and arrival at the final destination, allowing the evaluation of the operational efficiency of the system. This modeling framework incorporates stochastic variability in traffic conditions and enables an assessment of how different structural configurations of the network influence travel times and passengers' distribution.

The simulation framework is formally defined over the directed weighted graph $G = (V, E)$, where

- V represents the set of nodes corresponding to road intersections, bus stops, or relevant transport infrastructure points;

- E represents the set of directed edges corresponding to road segments connecting nodes, each associated with attributes such as physical length ℓ_{ij} and estimated travel time t_{ij}.

Each bus follows a predetermined route defined as an ordered subset of nodes $R = \{v_0, v_1, \ldots, v_n\} \subseteq V$, representing the full trajectory from origin to destination. The temporal dynamics of the trip are determined by two main components: Travel time between consecutive nodes and stopping time at intermediate stations. Thus, the total travel time T of a route is computed as

$$T = \sum_{i=0}^{n-1} \frac{\ell_{v_i v_{i+1}}}{v_i} + \sum_{i=0}^{n-1} \tau_{v_i}, \tag{2.2}$$

where

- $\ell_{v_i v_{i+1}}$ represents the length of the edge connecting nodes v_i and v_{i+1}, obtained directly from the `length` attribute of the road graph;

- v_i denotes the average speed of the bus on the corresponding road segment, randomly selected from a predefined interval associated with each geographic zone;

- τ_{v_i} represents the stopping time at node v_i, determined stochastically by passenger boarding and alighting dynamics and constrained by the maximum vehicle capacity.

Boarding time typically ranges between 10 and 30 seconds per passenger. This interval was established from field observations conducted on intermunicipal bus routes in the department of Quindío. The observed variability reflects the operational conditions of rural transportation, where passengers frequently board with luggage, agricultural products, or bulky personal belongings, increasing boarding times compared with those typically reported for urban public transport. Passenger alighting generally requires considerably less time because fare payment is completed during boarding; therefore, only the boarding process is explicitly incorporated into the service time estimation.

This model integrates the topological structure of the road network with the dynamic operational behavior of the public transport system, allowing the representation of realistic operating conditions such as travel time variability, passenger demand fluctuations, and service times. Based on this formulation, multiple simulation scenarios can be performed to evaluate the performance and robustness of the transportation system.

3. Results

3.1. Degree centrality analysis in the Quindío road network

Degree centrality is one of the most widely used metrics for analyzing complex networks, including road networks. For a node $v \in V$, degree centrality is defined as

$$C_D(v) = \deg(v), \tag{3.1}$$

where $\deg(v)$ represents the number of edges incident to node v. In directed graphs, two types are distinguished:

- **In-degree centrality**: Measures the number of incoming edges to a node, reflecting the amount of received connectivity;
- **Out-degree centrality**: Measures the number of outgoing edges from a node, indicating the number of connections generated by the node toward other nodes.

This indicator is useful for identifying nodes that function either as *arrival points* (important destinations) or *origin points* (traffic distributors) within the road network, and is typically associated with transport terminals, key intersections, or strategic corridors [11, 12, 40].

The analysis of the Quindío road network reveals relevant patterns with respect to these two centrality measures. Figure 3(a), corresponding to in-degree centrality, shows that nodes with the highest values tend to be concentrated in centrally connected areas, acting as the main destinations within the network. Peripheral nodes, by contrast, exhibit low values, indicating lower attraction of traffic flow.

Figure 3(b), which represents out-degree centrality, displays a similar spatial pattern but emphasizes nodes that act as generators of trajectories toward different sectors of the network. Together, both indicators make it possible to identify critical nodes for mobility optimization and intermunicipal public transport planning.

The distributions of in-degree and out-degree shown in Figure 3(c),(d) indicate that most nodes have low degree values, whereas only a few nodes exhibit higher connectivity. This pattern is consistent with the behavior typically observed in spatial road transportation networks, where geographical and infrastructural constraints limit nodes' connectivity and prevent the emergence of highly connected hubs. More specifically, nodes with degree three were found to be the most frequent, whereas nodes with degree five are less common. A considerable number of degree-one nodes were also identified, corresponding to road endpoints or dead-end segments where vehicles must return because no additional roads are available for further progression. Therefore, the observed degree distribution is more representative of a spatial transportation network than of a scale-free network characterized by a power-law degree distribution.

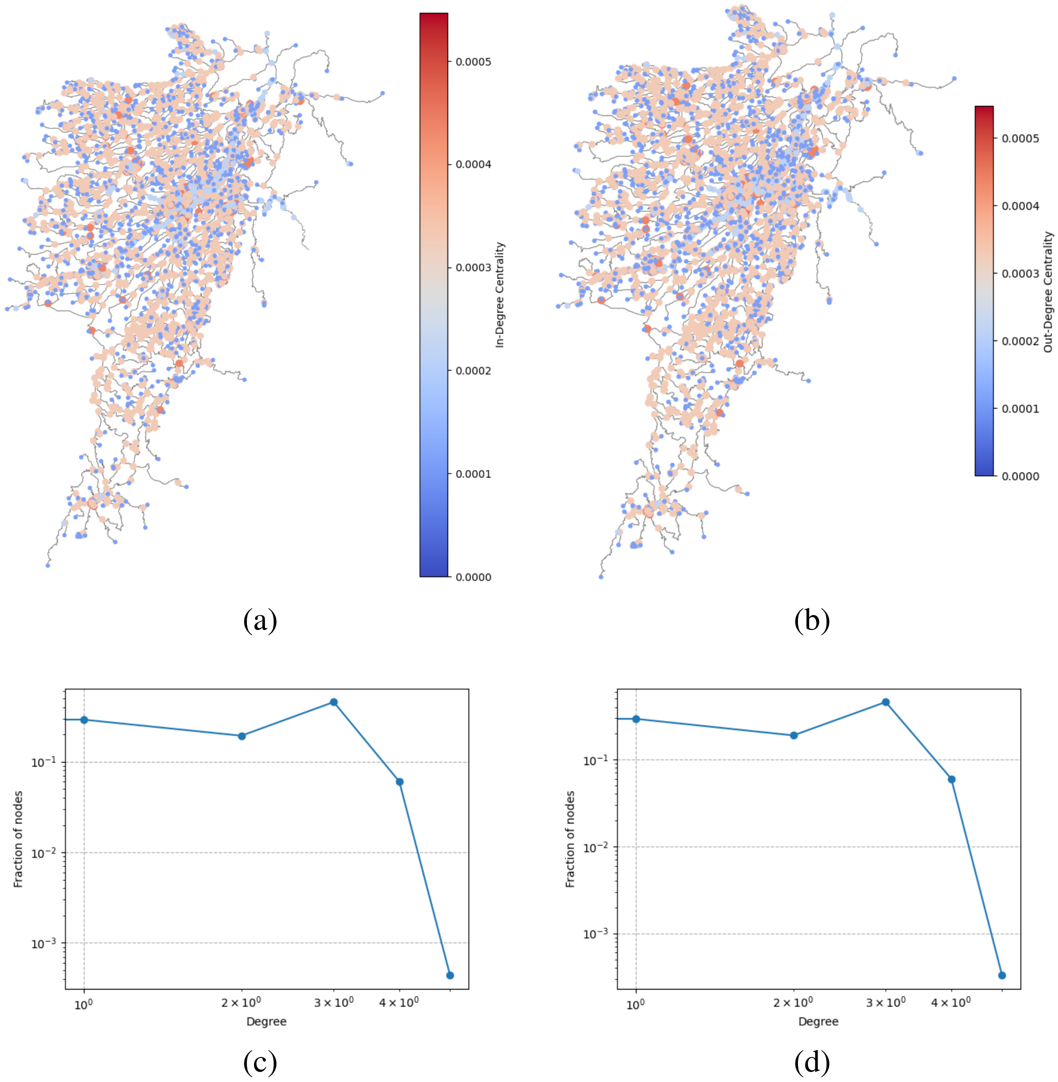

Figure 3. (a) In-degree centrality; (b) out-degree centrality; (c) distribution of in-degree values; (d) distribution of out-degree values.

3.2. *Closeness centrality*

Closeness centrality measures how close a node is to all other nodes in the network by computing the inverse of the sum of the shortest distances from that node to all others. For a node v, it is defined as

$$C_C(v) = \frac{N-1}{\sum\limits_{u \in V,\, u \neq v} d(v,u)}, \tag{3.2}$$

where

- N is the total number of nodes in the network;
- $d(v,u)$ is the shortest geodesic distance between node v and node u.

This metric is particularly useful for identifying nodes that can rapidly transmit information, traffic, or influence to other nodes. In the context of the Quindío road network, nodes with high closeness centrality are those with faster access to the rest of the network, suggesting that they may function as strategic centers for mobility and traffic distribution [12, 13, 40, 41].

Figure 4(a) presents the distribution of closeness centrality values. Most nodes exhibit relatively low centrality, which is typical of road networks in which only a small number of nodes occupy privileged positions for rapidly connecting different parts of the system. However, the upper tail of the distribution reveals the presence of a few nodes with significantly higher values, confirming the existence of key nodes that enhance the overall network connectivity. These findings are consistent with expectations for transportation networks, in which connectivity is unequally distributed and favors a limited number of strategic nodes.

Figure 4(b) shows the spatial distribution of closeness centrality in the Quindío road network. The highest values are mainly concentrated in the central part of the department, where the road density is greater. This concentration indicates that nodes in this area have better accessibility to other points in the network, suggesting that they are essential for the connectivity of the road system. Toward the territorial extremes, closeness centrality decreases, reflecting lower connectivity and larger average distances to other nodes.

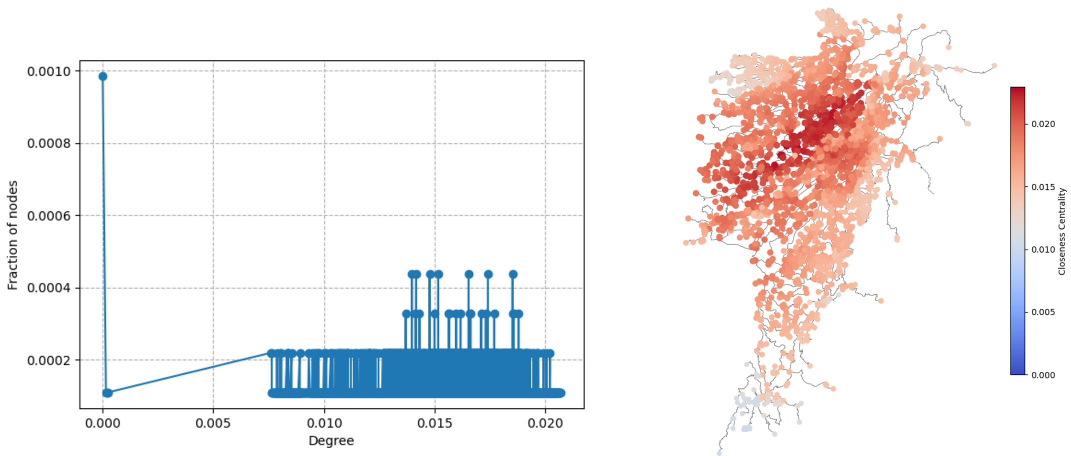

(a) (b)

Figure 4. Closeness centrality in the road network of the department of Quindío: (a) Distribution of closeness values; (b) geographic location of closeness centrality in the road network.

The analysis further indicates that the lowest closeness centrality values are located predominantly in the southern zone, corresponding to the municipality of Génova, and in the northwestern zone of the department. These sectors present lower relative accessibility due to their peripheral geographic position and the lower density of road connections linking them to the rest of the network. In particular, Génova, located in a mountainous and remote area, exhibits longer paths to other nodes in the network, reducing its efficiency in reaching different parts of the system. A similar pattern is observed in the northwestern zone, which is less integrated with the main road corridors and therefore requires longer routes to access other strategic nodes of the road network.

3.3. Betweenness centrality in the Quindío road network

Betweenness centrality is a metric that measures the frequency with which a node or an edge appears on the shortest paths between pairs of nodes in a network. This measure is especially useful for identifying nodes and edges that function as bridges or critical points for maintaining network connectivity [40, 42, 43].

For a node $v \in V$, betweenness centrality is defined as

$$C_B(v) = \sum_{\substack{s,t \in V \\ s \neq v \neq t}} \frac{\sigma_{st}(v)}{\sigma_{st}}, \tag{3.3}$$

and for an edge $e \in E$, as

$$C_B(e) = \sum_{\substack{s,t \in V \\ s \neq t}} \frac{\sigma_{st}(e)}{\sigma_{st}}, \tag{3.4}$$

where

- σ_{st} is the total number of shortest paths between s and t;
- $\sigma_{st}(v)$ is the number of those paths that pass through node v;
- $\sigma_{st}(e)$ is the number of those paths that pass through edge e.

In the context of the Quindío road network, nodes and edges with high betweenness centrality are fundamental for traffic flow, since their disruption could generate a significant impact on the overall connectivity of the system.

Figure 5(a) presents the spatial distribution of betweenness centrality for nodes in the Quindío road network. Contrary to what might be expected, the highest values are not concentrated exclusively on the major highways of the department. Instead, several road corridors stand out that, although not primary highways, play a key role in regional connectivity. These corridors include:

- **Montenegro–El Caimo–La Tebaida route**: A paved road with limited capacity and susceptibility to bottlenecks;
- **Calarcá–Armenia via Bohemia route**: A tertiary road with unpaved sections and structural limitations for heavy traffic;
- **Génova–Barragán–Armenia route**: The only paved road connecting Génova for all types of traffic;
- **Circasia via Montenegro and Circasia–Armenia via Hojas Anchas routes**: Paved roads requiring widening to improve their capacity;
- **Barcelona–Armenia via the "Y" junction**: a paved highway-type corridor that is crucial for connecting Valle del Cauca with Bogotá.

Figure 5(b) shows edge betweenness centrality, which evaluates the role of edges within the road network. The results also highlight the relevance of these secondary roads, which, despite not being formally classified as main roads, function as strategic corridors for intermunicipal mobility. The high betweenness centrality values observed in these roads suggest that any interruption along them could significantly affect traffic flow, emphasizing the need to improve their infrastructure in order to reduce the risk of network collapse.

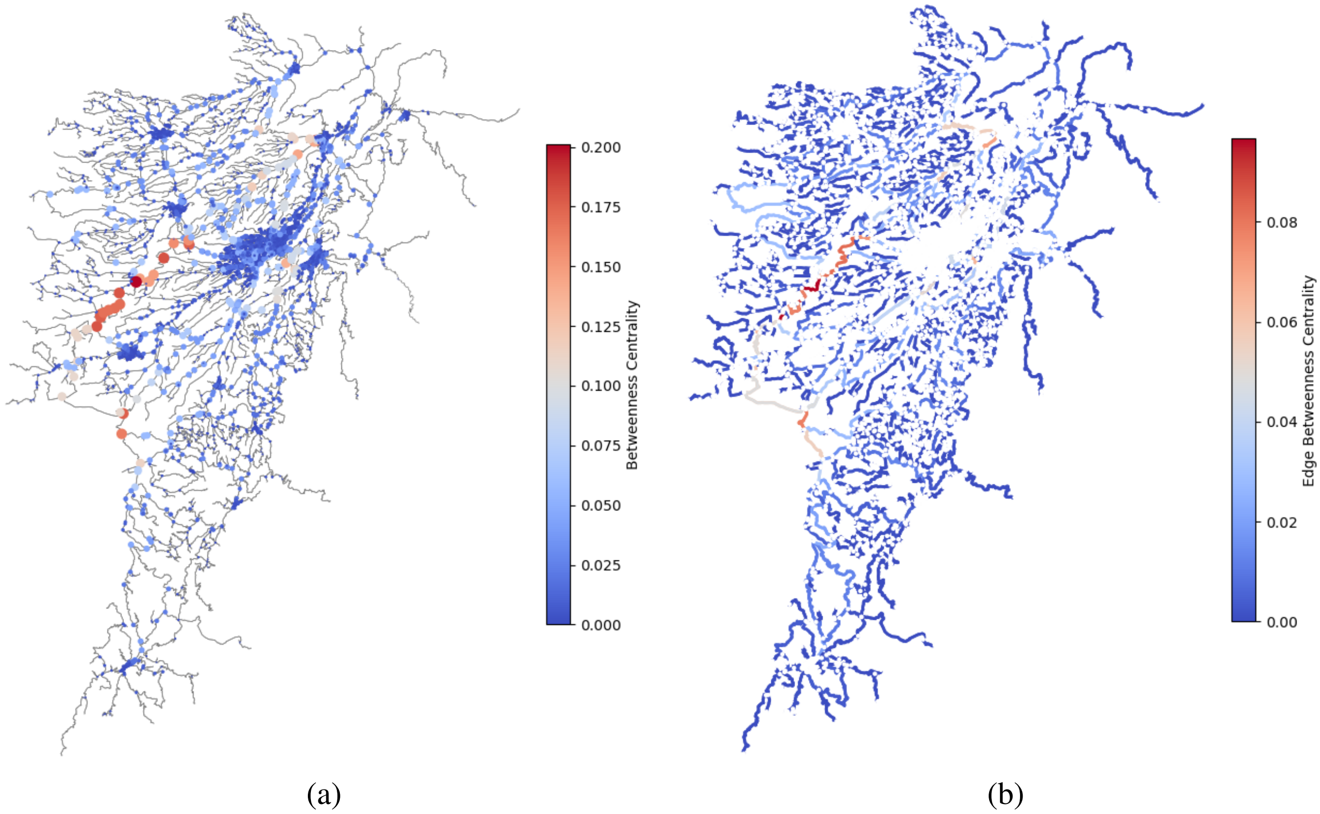

Figure 5. Betweenness centrality in the road network of the department of Quindío: (a) Node betweenness centrality; (b) edge betweenness centrality.

Figure 6 shows that, with the exception of the **Barcelona–Armenia via the Y junction route**, all the roads identified as critical are secondary corridors and exhibit high vulnerability to closures caused by severe weather, accidents, landslides, or other disruptive events. These findings indicate that betweenness centrality and edge betweenness centrality are effective for identifying routes whose structural integrity is essential for preserving regional connectivity. Consequently, these roads should be prioritized for capacity improvements and infrastructure reinforcement, including higher-quality asphalt layers and appropriate road signaling.

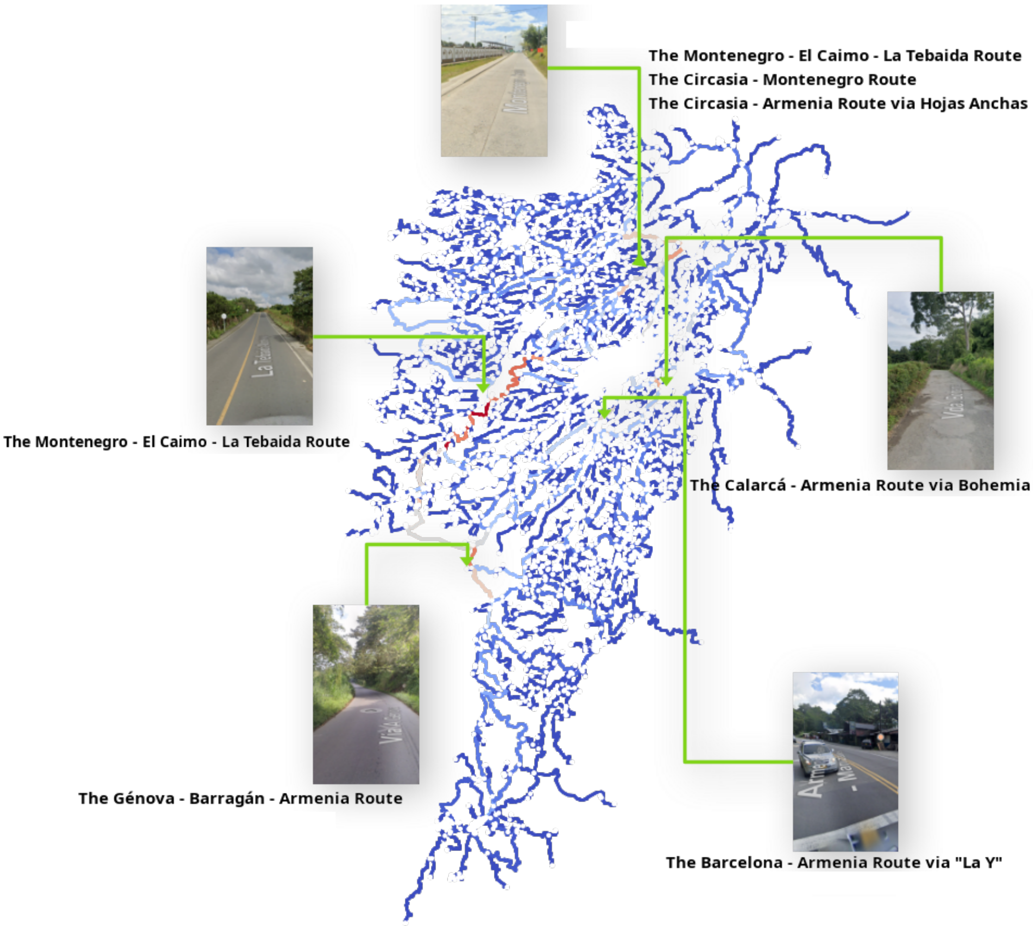

Figure 6. Road map of the department of Quindío and roads with the highest edge betweenness centrality values. Screenshot taken from `Google Maps`.

3.4. *Eccentricity in the public transport network*

The eccentricity of a node in a network is defined as the greatest geodesic distance between that node and any other node in the network [13, 44–46]. Mathematically, for a node v, its eccentricity $\varepsilon(v)$ is defined as

$$\varepsilon(v) = \max_{u \in V} d(v, u), \tag{3.5}$$

where $d(v, u)$ represents the shortest distance between nodes v and u in the graph $G = (V, E)$. This measure provides a way of evaluating how far a node may be from the rest of the network and is useful for identifying both central and peripheral nodes.

Figure 7 presents the spatial distribution of eccentricity in the road network of the department of Quindío. In this visualization, colors range from blue (low eccentricity) to red (high eccentricity). The radius of the network ($R = 85$) is also indicated, corresponding to the minimum eccentricity value, together with the diameter ($D = 139$), which represents the maximum distance between pairs of nodes.

Nodes with lower eccentricity, that is, those from which any other point in the network can be reached with shorter maximum distance, are concentrated in the central region of the department, particularly in the urban area of Armenia and its zone of influence. These areas may be considered *structural centers* of the road network and therefore constitute suitable locations for critical transport infrastructure such as intermunicipal terminals or logistics centers.

By contrast, nodes with higher eccentricity values (red zones in the figure) are located in the northern, eastern, and southern extremes of Quindío, especially in rural or difficult to access areas such as the district of Barragán or rural roads toward Génova. These areas are farther from the functional center of the network and require more time or distance to connect with the rest of the system, making them more vulnerable to isolation, and are therefore priority targets for strategies aimed at improving connectivity or providing complementary transport services.

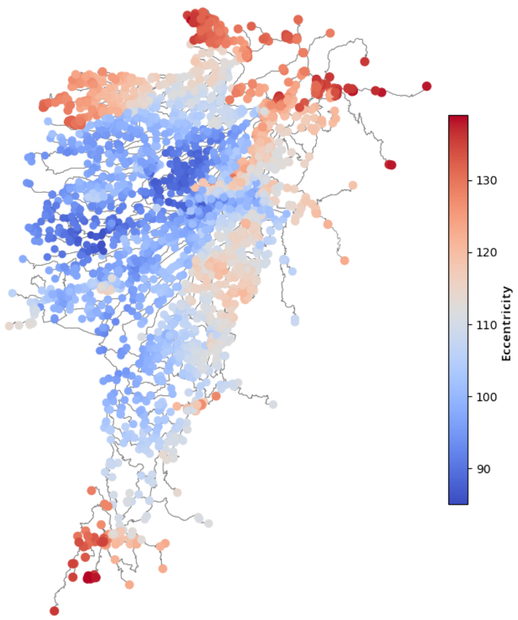

Figure 7. Eccentricity in the Quindío transport network. The minimum radius $R = 85$ and the diameter $D = 139$ are highlighted. Nodes in blue have lower eccentricity (central zones), whereas nodes in red indicate higher eccentricity (peripheral zones).

3.5. *Eigenvector centrality*

Eigenvector centrality is a metric that quantifies the structural importance of a node as a function of both its connectivity and the importance of its neighbors. Unlike degree centrality, which simply counts direct connections, eigenvector centrality assumes that connections to influential nodes increase the prestige of the evaluated node [47–49]. This measure is defined as the solution of the system

$$\vec{x} = \lambda A \vec{x}, \tag{3.6}$$

where A is the adjacency matrix of the graph, $\vec{x}$ is the vector of node centralities, and λ is the largest associated eigenvalue. The value x_i for each node i reflects its relative importance in the network.

Figure 8 shows the spatial distribution of eigenvector centrality in the road network of the department of Quindío. Nodes are coded by color (from blue to red) and size, where higher values indicate structurally influential nodes surrounded by other highly connected nodes.

The figure shows that nodes with the highest centrality values cluster in the metropolitan area of Armenia, where connection density and route redundancy are greater. These nodes act as concentration points for potential flow in the network and can therefore be regarded as essential for the stability and efficiency of the intermunicipal transport system.

In contrast, nodes with low eigenvector centrality are located in peripheral and rural areas, where connectivity is sparse or dominated by terminal routes. Although these points may remain operationally active, they exert limited structural influence on the rest of the network, and their disconnection would have a smaller impact on the overall integrity of the system.

Eigenvector centrality complements other metrics such as betweenness and eccentricity, since it reveals not only how connected a node is but also how strategically positioned it is within the hierarchical structure of the network.

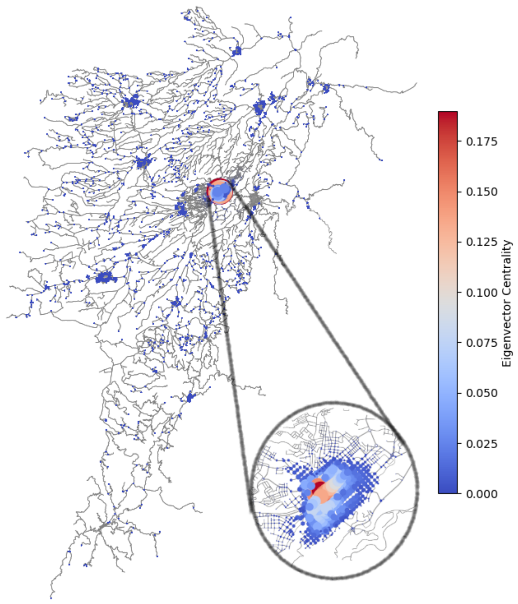

Figure 8. Eigenvector centrality in the Quindío road network. The most central nodes appear in red, whereas peripheral nodes are shown in blue. The inset circle highlights that the central area of the city of Armenia contains the most central nodes in the network.

3.6. Straightness centrality

Straightness centrality is a metric that evaluates the geometric efficiency of access from a node to the rest of the network. It is defined as the ratio between the Euclidean distance (straight-line distance) and the geodesic distance (actual distance along the network) between pairs of nodes. For a node i, straightness centrality is expressed as

$$SC(i) = \frac{1}{N-1} \sum_{\substack{j \in V \\ j \neq i}} \frac{d_E(i,j)}{d_G(i,j)}, \tag{3.7}$$

where $d_E(i, j)$ is the Euclidean distance between nodes i and j, and $d_G(i, j)$ is the geodesic distance along the network. This metric takes values between 0 and 1, with 1 representing perfectly direct paths. Straightness centrality was proposed to analyze the efficiency of movement in spatial networks and has been successfully applied in urban and mobility studies [29, 50, 51].

In the context of public transportation, this measure makes it possible to identify nodes that provide relatively direct routes to many other points in the system, and it is associated with greater spatial accessibility. A node with high straightness centrality represents a structurally privileged location for optimizing passenger mobility and reducing travel times.

Figure 9 presents the spatial distribution of straightness centrality in the road network of the department of Quindío, based on the previously computed values. Nodes in red indicate high straightness values, whereas nodes in blue reflect lower geometric efficiency.

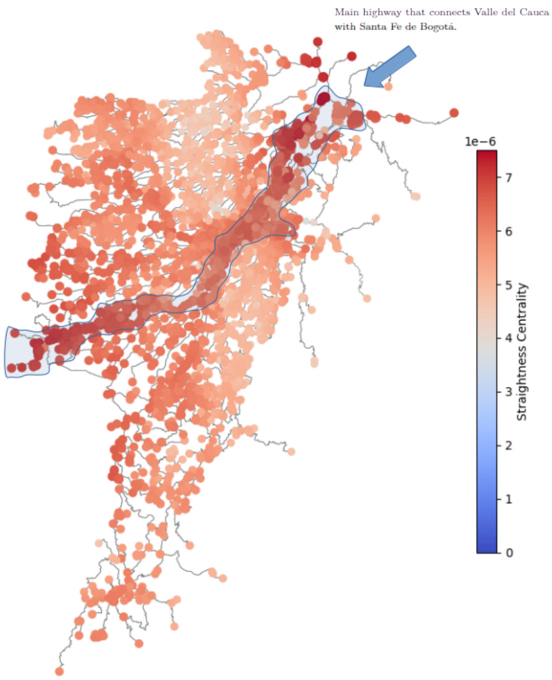

Figure 9. Straightness centrality in the Quindío road network. Nodes in red indicate more direct trajectories with respect to the rest of the network.

As shown in Figure 9, nodes with higher straightness centrality tend to cluster in the central region of the department, particularly around the highway that enters from the department of Valle del Cauca and crosses Quindío from southwest to northeast, continuing toward the departments of Risaralda and Tolima. A similar pattern is observed around the metropolitan area of Armenia, where the road network is denser and more structured. These nodes provide relatively direct access to multiple sectors of the territory, making them highly efficient locations for public transport operations.

By contrast, nodes with low straightness centrality are concentrated mainly in the northern extreme, particularly on rural roads crossing the Barbas Bremen natural reserve, as well as in the southern and eastern sectors of Quindío, where local mountain roads in the Central Andes are characterized by indirect trajectories, winding routes, and limited connectivity.

3.7. Percolation-based resilience assessment in the road network

To evaluate the structural resilience of the road network of the department of Quindío, a percolation-based analysis was performed. In this study, resilience is understood as the capacity of the network to preserve global connectivity under node removal processes, while percolation provides the methodological framework used to evaluate how this connectivity changes as nodes are progressively removed. Therefore, resilience assessment and percolation analysis are not treated as independent procedures but as complementary components of the same robustness analysis.

The road network extracted using the `OSMnx` library was represented as an undirected graph in order to simplify the structural connectivity analysis. The relative size of the giant component (that is, the largest connected component of the network) was used as the main indicator of global connectivity. Following the structural perspective proposed by Costa [36] and Paul et al. [37], two perturbation scenarios were considered:

1. **Targeted attack**: Sequential removal of nodes according to their structural importance, initially based on node degree;
2. **Random failure**: Removal of randomly selected nodes.

Percolation theory provides a formal framework for studying structural transitions in complex networks [52, 53]. Originally developed in statistical physics, this theory describes how, as an occupation parameter changes, such as the probability that a node or link is active, a network may transition from a connected state to a fragmented one. This phenomenon has been widely applied to evaluate the robustness, connectivity, and resilience of complex systems, including urban transportation networks [54–56].

In transportation networks, percolation analysis makes it possible to identify critical points beyond which the functional network loses global connectivity. The emergence or preservation of a giant component is interpreted as a signal of structural functionality, whereas fragmentation into small components represents a loss of global connectivity. Li et al. [57], for example, applied this framework to the road network of Beijing and showed that percolation-based indicators can identify structural bottlenecks that are not always captured by classical centrality measures.

In the first stage, the effect of moderate perturbations was evaluated by removing up to 50 nodes from the network. Under both the random and targeted removal scenarios, the evolution of the giant component was measured as nodes were removed. This made it possible to evaluate how the overall connectivity of the network decreases under localized perturbations.

Figure 10 shows that under moderate perturbations, both scenarios produce only a slight decline in connectivity. The targeted attack based on node degree leads to a gradual decrease in the size of the giant component, while the random failure scenario remains initially stable and then exhibits a more pronounced reduction after approximately 35 nodes have been removed. Nevertheless, in both cases, the giant component remains above 98.7% after the removal of 50 nodes. This indicates that the Quindío road network is robust against localized or moderate structural failures.

Resilience index based on the area under the curve (AUC)

To quantify this behavior, the area under the curve (AUC) was computed for each scenario. This index summarizes the stability of the giant component throughout the node removal process.

The results shown in Figure 10 and Table 1 suggest that, when only a small fraction of the total network is removed, the Quindío road network preserves most of its structural connectivity. The minimal difference between the AUC indices indicates that degree-based targeted attacks and random failures have similar effects at this perturbation scale. This behavior is consistent with the relatively homogeneous and bounded-degree structure of spatial road networks, where the node degree is constrained by geographical and infrastructural factors.

However, this result should not be interpreted as evidence that the network is globally resilient under all possible levels of disruption. The previous experiment evaluates only moderate perturbations, corresponding to the removal of a limited number of nodes. To examine the network's response under more severe disruptions, the node removal process was extended to larger fractions of the network through random and targeted percolation scenarios.

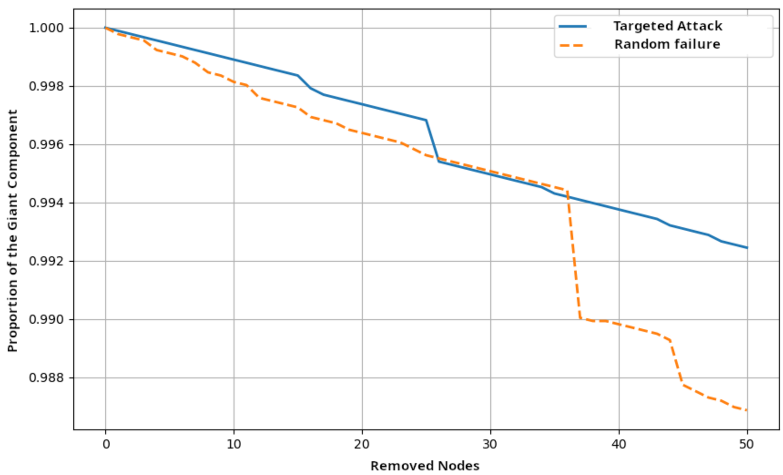

Figure 10. Evolution of the giant component under node removal.

Table 1. Structural resilience index according to the area under the curve.

Type of perturbation	Resilience index (AUC)
Targeted attack (by degree)	49.81
Random failure	49.73

3.7.1. Random percolation

As shown in Figure 11, the percolation curve under random node removal shows a progressive decrease in the proportion of the giant component as the fraction of removed nodes increases. Initially, the network preserves a highly connected structure. However, once approximately 10% of the nodes have been removed, an accelerated decline in overall connectivity becomes evident. When nearly 30% of the nodes are removed, the giant component shrinks to less than 10% of its original size, and by 50% removal, it practically disappears.

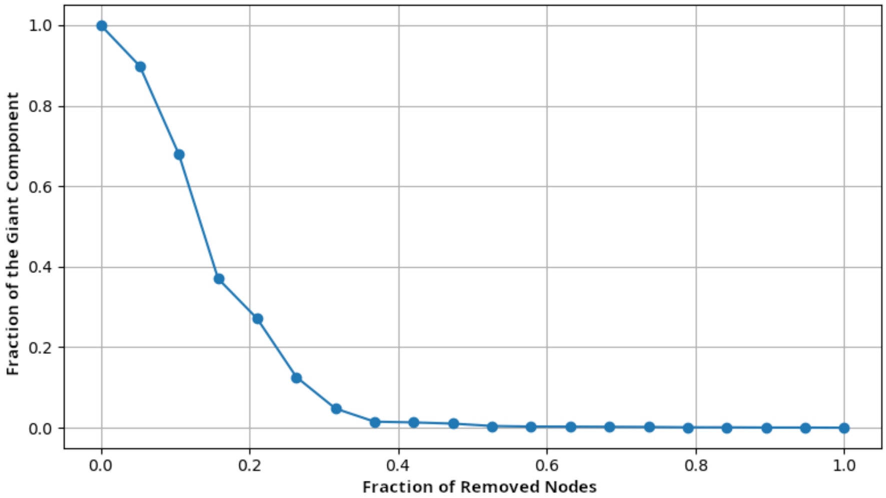

Figure 11. Percolation curve under random node removal.

The normalized resilience index calculated for this scenario was 0.16. This value reflects a substantial reduction in connectivity as node removal progresses. Although the network preserves its structure under moderate localized failures, large-scale random disruptions produce a significant decrease in the size of the giant component, indicating a progressive loss of global connectivity.

3.7.2. Targeted percolation

As shown in Figure 12, in the targeted percolation scenario, nodes were removed in decreasing order according to their degree. The corresponding curve shows slightly greater persistence of the giant component during the initial stages of node removal. Nevertheless, a significant reduction in connectivity is observed once approximately 10% of the nodes have been eliminated. Although the decline is more gradual than in the random case, the network still undergoes substantial fragmentation as the fraction of removed nodes increases.

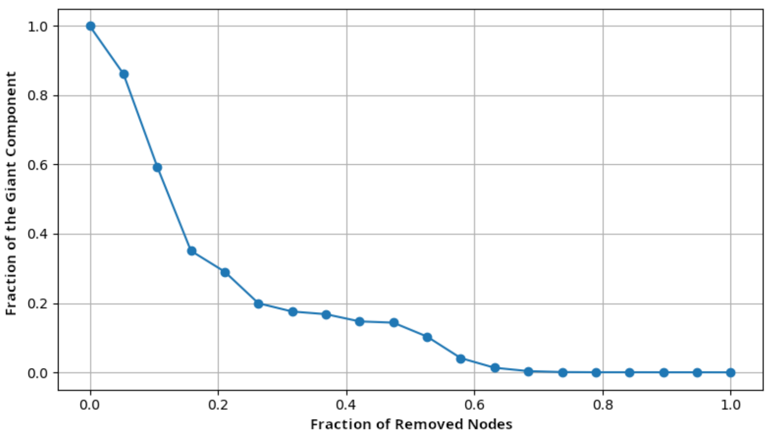

Figure 12. Percolation curve under targeted node removal.

The resulting normalized resilience index was 0.19, slightly higher than in the random percolation scenario. This suggests that network connectivity is not concentrated exclusively in a small subset of high-degree nodes, which is consistent with the structural characteristics of spatial road networks. Nevertheless, the progressive loss of connectivity under extensive node removal reveals that structural fragilities still persist.

Taken together, these results clarify the apparent contrast between the moderate node-removal experiment and the full percolation analysis. The Quindío road network should not be described as simply "resilient" or "fragile" in absolute terms. Rather, its behavior depends on the scale of the perturbation. The network is robust against localized or moderate failures, preserving most of its giant component when only a limited number of nodes have been removed. However, it becomes increasingly vulnerable under large-scale disruptions, where the accumulation of failures leads to global fragmentation.

This distinction is relevant for planning intermunicipal public transportation. Isolated incidents may be absorbed by the network without a major loss of structural connectivity, but widespread disruptions caused by landslides, extreme rainfall, simultaneous road closures, or deterioration of several secondary corridors may severely compromise regional accessibility. Therefore, percolation-based resilience assessment provides useful quantitative evidence for identifying the limits of the network's robustness and for prioritizing interventions aimed at improving redundancy and connectivity in vulnerable areas.

3.7.3. Percolation under different centrality-based attack strategies

To further investigate the structural vulnerability of the Quindío road network, percolation analyses were performed using three centrality-based attack strategies: Degree, betweenness, and closeness centrality. This comparison makes it possible to evaluate how different definitions of nodes' importance affect the network's robustness and to identify the nodes that play the most critical role in maintaining global connectivity.

For each strategy, nodes were sequentially removed in decreasing order of centrality, and the relative size of the giant component was monitored as a function of the fraction of removed nodes. The resilience of the network was quantified using the normalized percolation AUC, where lower values indicate a faster loss of connectivity and therefore greater vulnerability.

Figure 13 and Table 2 reveal substantial differences among the attack strategies. The most disruptive scenario corresponds to the removal of nodes with the highest betweenness centrality, producing a rapid collapse of the giant component and yielding the lowest resilience index (AUC = 0.065). This result indicates that the overall connectivity of the road network depends strongly on a relatively small number of bridging nodes that connect different sectors of the system.

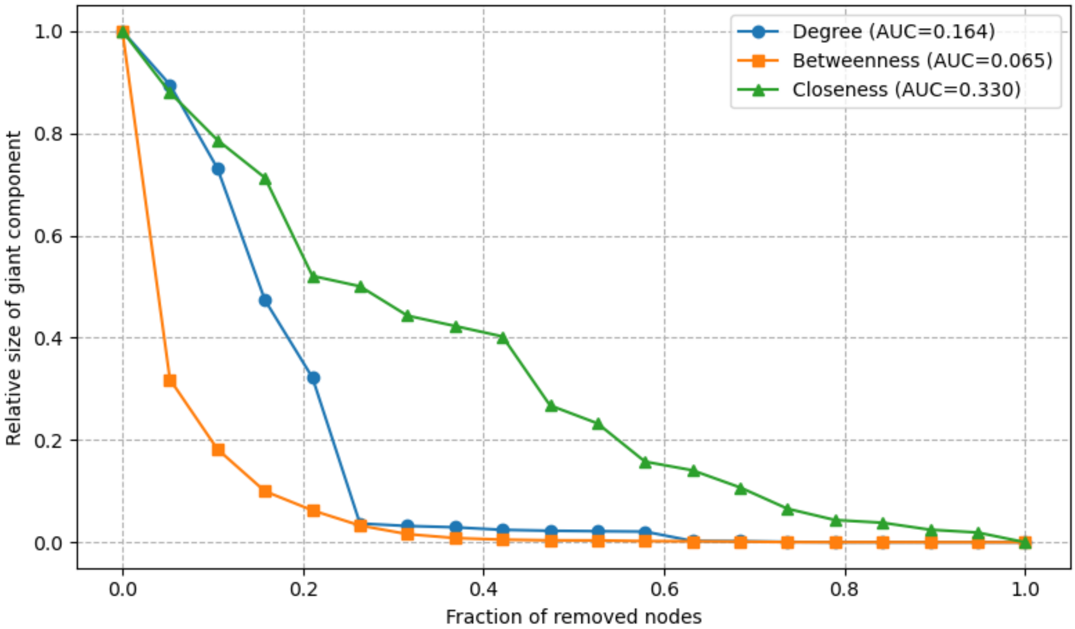

Figure 13. Percolation curves obtained under degree-betweenness, and closeness-based attack strategies.

Table 2. Resilience indices obtained for different attack strategies.

Attack strategy	Resilience index (AUC)
Degree centrality	0.164
Betweenness centrality	0.065
Closeness centrality	0.330

The attack based on degree centrality also reduces connectivity, but its impact is considerably weaker (AUC = 0.164). This behavior suggests that the number of direct connections of a node is not the most informative indicator of structural importance in this road network. Since most intersections exhibit similar degree values, removing the highest-degree nodes does not immediately fragment the system.

In contrast, the closeness-based attack produces the highest resilience index (AUC = 0.330), indicating that nodes with high accessibility are not necessarily the most critical for preserving global connectivity. Although their removal increases travel distances and reduces efficiency, the network remains structurally connected for a longer period.

These results demonstrate that betweenness centrality is the most effective metric for identifying critical nodes in the Quindío road network. Consequently, the network's vulnerability is associated primarily with intermediary nodes that act as bridges between regions rather than with highly connected nodes. This finding is consistent with previous studies on transportation systems, where structural robustness is often governed by corridor-like elements that concentrate the shortest paths and traffic flows [54, 55, 57].

The comparison also highlights the importance of evaluating multiple centrality measures when assessing transportation network resilience. While degree centrality provides information about local connectivity, betweenness centrality captures the strategic role of nodes in maintaining global accessibility and therefore offers a more suitable criterion for vulnerability analysis in spatial road networks.

3.8. Public transport simulation

The discrete event simulation is directly coupled with the road network obtained from the complex network analysis. The road graph is not used solely for topological characterization; it provides the feasible transportation corridors, the travel distances between origin and destination, and the set of alternative routes available under road disruption scenarios. Consequently, the simulation operates on the transportation network extracted from the graph, allowing structural changes in the network to be translated into measurable operational impacts. Travel times are therefore not determined exclusively by the geometric length of the routes, but also by stochastic operating conditions, including speed variations along different road segments and passenger boarding and alighting processes.

A simulation was then performed on a route that the centrality analysis had identified as sensitive to interruptions.

3.8.1. Génova–Armenia transport terminal route

Figure 14 shows the route followed by the bus in the simulation, connecting the municipality of Génova with the transport terminal of the city of Armenia. This route crosses the department from south to north and was used to evaluate passengers' boarding and alighting dynamics, as well as travel times and cumulative distance.

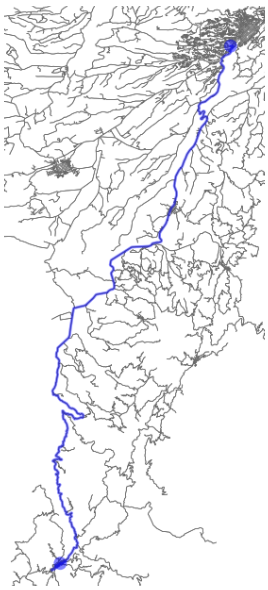

Figure 14. Simulated bus route from Génova to Armenia.

During the simulation, the bus started with a partial load of 10 passengers. In terms of distance, the simulated trajectory accumulated a total of 53,963.02 meters (approximately 54 km).

To evaluate travel-time variability and compare it with real-world estimates, 100 independent simulations of the route were performed, and the results are shown in Figure 15. Each point in the graph represents the total travel time (in minutes) required for the bus to complete the route in one simulation run, taking into account random events such as the speed in each segment, the number of passengers boarding and alighting, and the time required for each operation. The green dashed line indicates the average simulated travel time, approximately 96.90 minutes, while the red line represents the travel time estimated by Google Maps, which is 84 minutes for the same route.

The travel time reported by Google Maps (84.00 min) was used only as an external operational reference rather than as a formal calibration dataset. This value corresponds to a weekday estimation obtained under normal traffic conditions and provides an independent benchmark for assessing the realism of the simulated travel times. Since the objective of the proposed model is to evaluate the operational effects of the road network topology and stochastic service variability, rather than to reproduce the traffic conditions of a specific day, the comparison should be interpreted as an indication of the model's consistency rather than as a direct validation against GPS trajectories collected from transport operators.

This analysis shows that although there is inherent variability in the travel times due to factors such as speed fluctuations across road segments and passengers' boarding and alighting dynamics, the simulated model produces an average travel time reasonably close to the real estimate. It should be noted that, although Google Maps includes an option for public transport times, this functionality is not enabled for intermunicipal routes in the department of Quindío. For this reason, the estimate based on private vehicle travel time was adopted as the reference.

Despite this limitation, Figure 15 shows that the difference between the average simulation time (green dashed line) and the Google Maps estimate (red line) remains within a range of approximately 10 to 12 minutes. This difference can be mainly attributed to the operational stops required by public transport for passengers' boarding and alighting.

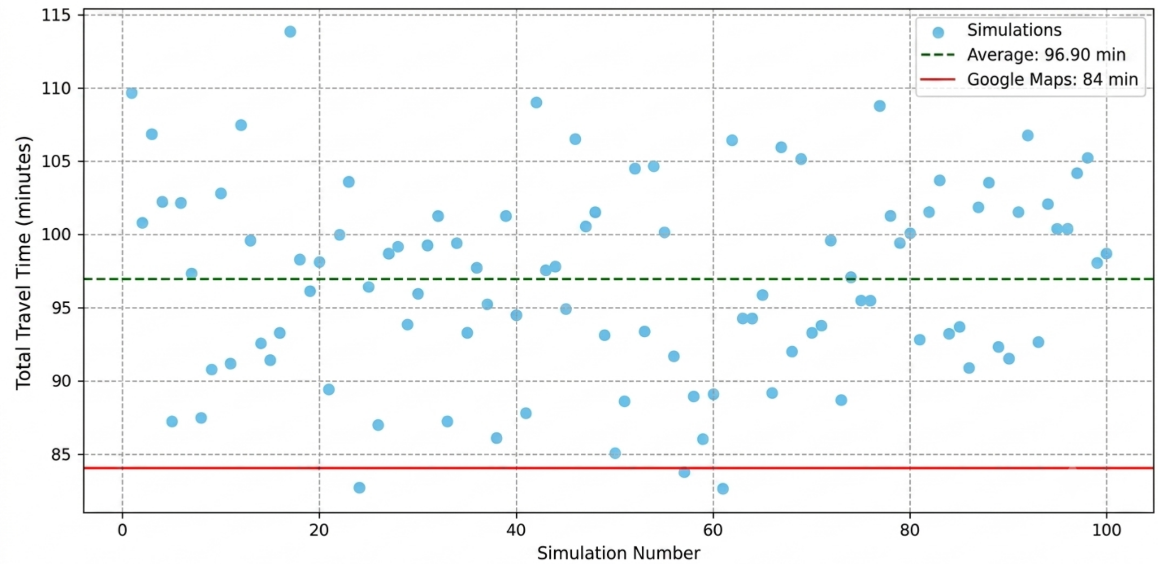

Figure 15. Dispersion of simulated travel times compared with the travel time estimated by `Google Maps`.

3.8.2. Simulation of decision-making under road disruptions: Génova–Armenia case

This experiment illustrates the integration between complex network analysis and discrete event simulation. After identifying a structurally sensitive corridor through the network analysis, a disruption is introduced into the road graph. The resulting feasible alternative routes are then obtained from the underlying network topology and evaluated through simulation to quantify their operational consequences in terms of travel time and route performance.

One of the fundamental aspects of intermunicipal public transport planning is the capacity to adapt to unexpected road interruptions. In order to analyze this capability in the road network of the department of Quindío, a decision-making simulation was carried out based on a critical disruption on the usual route connecting the municipality of Génova with the Armenia transport terminal. This interruption was simulated in the road segment known as the "Y" descent, an area historically associated with a high incidence of traffic accidents.

The usual route from Génova to the Armenia Terminal covers a distance of 53.96 km, passing through Barragán, Barcelona, and the direct road toward the city of Armenia. Figure 16(a) shows the geographic layout of this route, whereas Figure 16(b) illustrates the dispersion of travel times obtained from 100 simulations. The average simulated time was approximately 96.90 minutes, while the corresponding Google Maps estimate for the same route is 84 minutes.

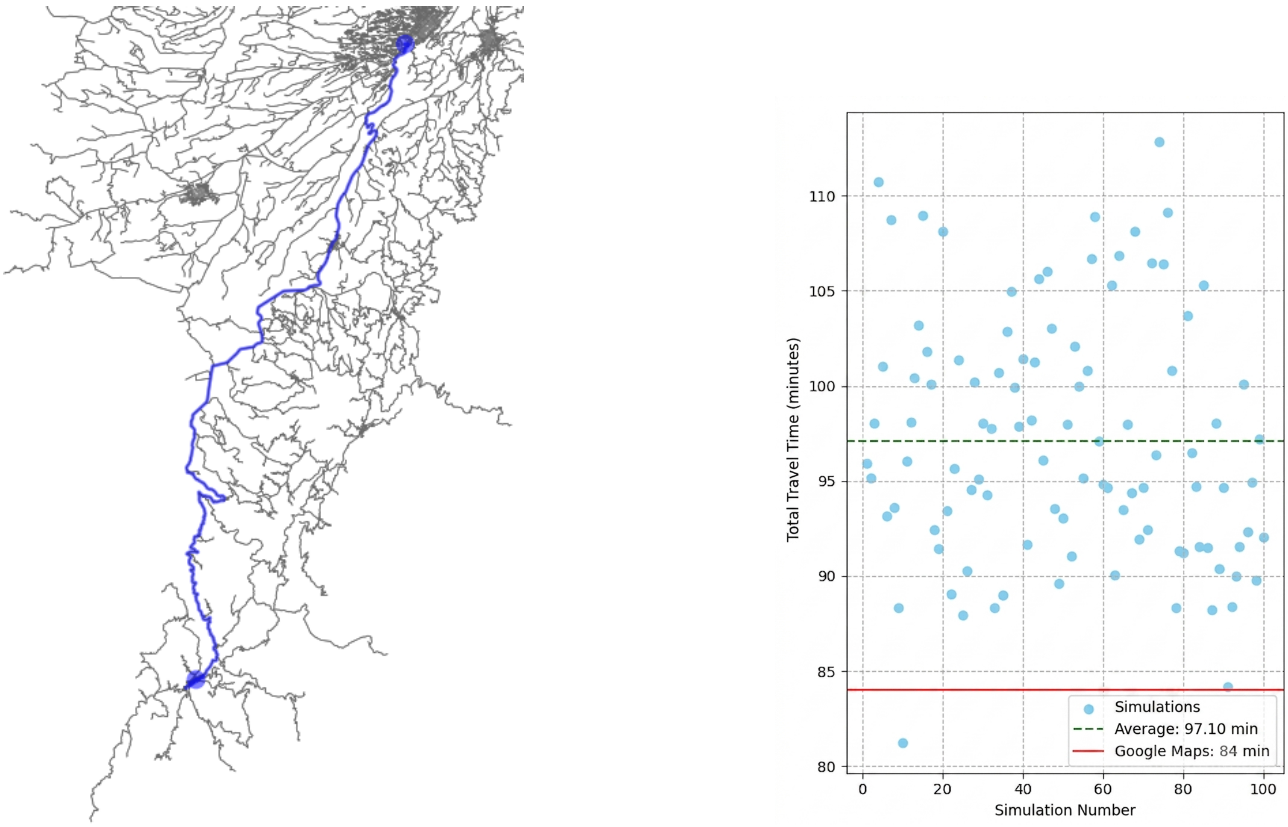

(a) Usual Génova–Armenia route (53.96 km)

(b) Travel time simulation for the usual route

Figure 16. Route and travel time simulation for the usual trip between Génova and Armenia.

Given the simulated interruption at the "Y" sector, two feasible alternative routes were identified from the road network and subsequently evaluated through discrete event simulation. The first alternative (Calarcá-Terminal) follows the main corridor toward the city of Calarcá, a highway that connects Valle del Cauca with Bogotá. Along this route, the bus bypasses the urban area of Calarcá and continues toward the roundabout on the road to Ibagué, finally taking the road toward Armenia and reaching the terminal. This route has a total length of 63.54 km, representing an increase of approximately 9.58 km with respect to the usual route. Figure 17(a) presents the route map, and Figure 17(b) shows the simulation results, with an average travel time of 104.63 minutes. This represents an additional travel cost of approximately 10 minutes and is very close to the Google Maps estimate of 103 minutes.

(a) Alternative route via Calarcá (63.54 km)

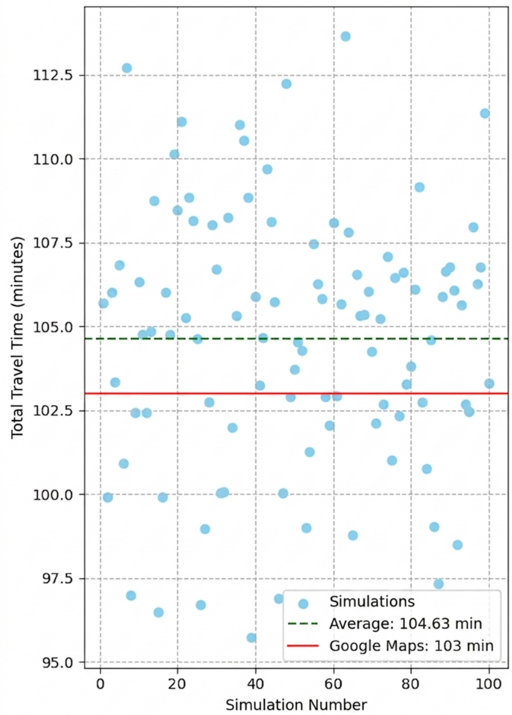

(b) Travel time simulation for the route via Calarcá

Figure 17. Alternative route and travel-time simulation for the Génova–Armenia trip via Calarcá.

The second alternative considers a route through the municipality of La Tebaida (Tebaida–Terminal). The bus descends along a tertiary road, which is unpaved in some sections, toward the roundabout leading to El Edén International Airport. From there, it takes a modern dual carriageway directly to the city of Armenia. This is arguably one of the highest-quality roads in the department. The total distance of this route is 55.67 km, only 1.71 km longer than the usual route. Figure 18(a) shows the geographic trajectory, whereas Figure 18(b) presents the resulting travel time dispersion, with an average of 122.48 minutes.

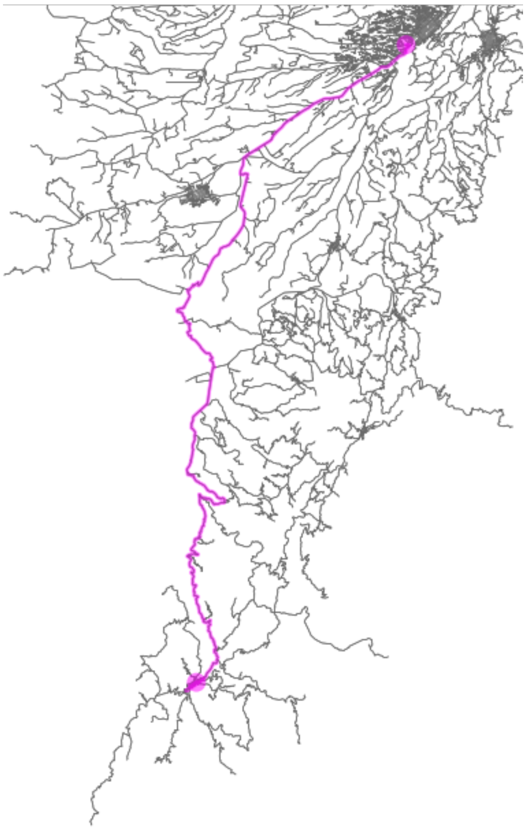

(a) Alternative route via La Tebaida (55.67 km)

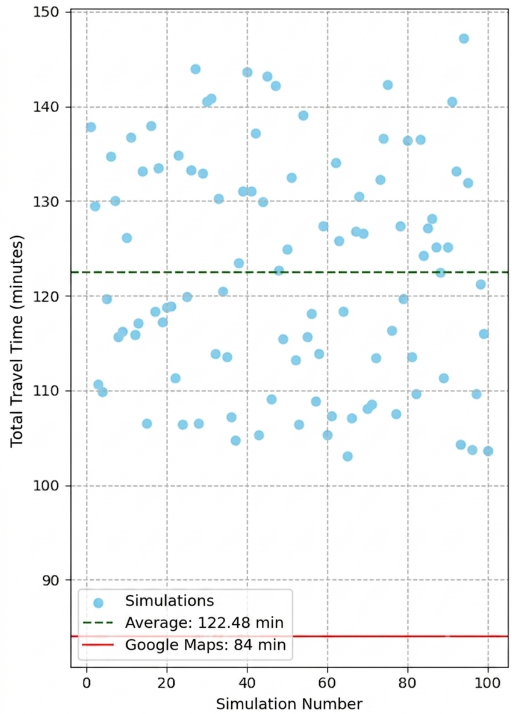

(b) Travel time simulation for the route via La Tebaida

Figure 18. Alternative route and travel time simulation for the Génova–Armenia trip via La Tebaida.

The obtained results show that during an interruption of the usual Génova–Armenia route, the Quindío road network provides viable alternatives, although at the cost of a significant increase in travel time. The usual route registers an average time of 95.73 minutes, whereas the alternative route via Calarcá increases this value by approximately 9 minutes, yielding an average of 104.63 minutes. In turn, the alternative route through La Tebaida produces an average time of 122.48 minutes, corresponding to an increase of approximately 27 minutes with respect to the main route. These results indicate that, although the system offers redundancy in connectivity, the alternative routes imply substantial temporal costs from the perspective of intermunicipal transport decision-making and road planning.

It is important to clarify that, although the second alternative (Tebaida–Terminal) presents a distance only slightly longer than the usual route, its viability is strongly conditioned by the physical state of the road in its initial section, namely the initial detour from the traditional route. As shown in Figure 19, this sector is unpaved and lacks adequate infrastructure, which could hinder the circulation of heavy vehicles such as intermunicipal buses, especially during rainy periods. In fact, Google Maps does not enable this route under the public transport option for this area, and in Figure 18(b), the usual route was therefore kept as the reference. Consequently, although the computational simulation yields feasible results, albeit with longer travel times, this route requires a more careful practical assessment before it can be considered a safe and efficient alternative under disruption scenarios.

Figure 19. Road conditions on the Génova–Armenia transport terminal alternative route via La Tebaida.

After the first section of the Tebaida–Terminal route, which is not suitable for public transport circulation, the route continues along a road that can be considered one of the best in the department of Quindío, characterized by a dual carriageway infrastructure and higher operating speeds. These conditions partially compensate for the delays generated in the initial section of the route.

It is also important to note that, in both alternative scenarios, the model did not include passenger boarding or alighting events because the simulations represent an emergency rerouting scenario caused by an unexpected road disruption. Under these circumstances, buses are assumed to continue transporting only the passengers already on board at the moment of the incident, while the probability of new passengers boarding or alighting along the temporary diversion routes is considered negligible. This assumption allows the analysis to isolate the impact of the route diversion on travel times and network performance without introducing additional variability associated with passenger demand.

In summary, the simulation results indicate that, under interruptions on the usual route between Génova and Armenia, the most efficient operational option is to redirect traffic through the Calarcá–terminal corridor. Although this route is slightly longer in terms of distance, it represents an increase of only 9 minutes with respect to the usual trip, compared with more than 25 additional minutes for the route via La Tebaida. This difference is critical in contexts where arrival time, service efficiency, and traffic flow optimization are determining factors for intermunicipal public transport operators. In addition, the route through Calarcá runs along paved, high-capacity primary roads, which reduces risks associated with road infrastructure's condition, passenger safety, and vehicle wear.

Overall, the proposed framework combines structural network analysis with discrete event simulation to support operational decision-making in intermunicipal transportation. The complex network provides the topological representation of the road system, identifies structurally sensitive corridors, and determines feasible alternative routes, whereas the simulation quantifies the operational consequences of these structural changes. This integration enables the evaluation of disruption scenarios from both topological and transportation perspectives.

4. Conclusions

In general terms, the methodological framework developed in this study demonstrates that the integration of complex network theory with discrete event simulation models based on queueing theory constitutes a powerful and versatile approach for analyzing interurban passenger public transportation systems. Representing transport systems as graphs allows rigorous characterization of the topological structure of the road network, enabling the identification of critical elements and the evaluation of their resilience under perturbations. At the same time, discrete event simulation makes it possible to model the operational dynamics of passenger flows, incorporating the inherent variability associated with travel times, service frequencies, and passenger boarding and alighting processes.

This methodological combination provides an integrated perspective that goes beyond purely macroscopic or static approaches, offering realistic estimates of the system's performance under different scenarios. Due to its modular and scalable nature, the proposed framework can be adapted to different territorial contexts and levels of complexity, making it a generalizable tool for the planning, evaluation, and management of interurban public transportation systems in diverse regions and mobility networks.

An important contribution of the proposed framework is that the complex network and the discrete event simulation are not treated as independent analytical stages. Instead, the road network directly constrains the operational simulation by determining feasible routes, travel distances, intermediate stopping locations, and the response to disruption scenarios. Consequently, structural modifications to the network are immediately translated into measurable operational impacts, establishing an explicit connection between topological vulnerability and transportation performance.

The department of Quindío in Colombia was selected as a case study. The results of the centrality analysis reveal a strongly hierarchical road structure characterized by the presence of critical nodes and corridors that concentrate a significant proportion of the connectivity and potential flow of the system. Degree and closeness centrality metrics identified a strong concentration of connectivity around the metropolitan area of Armenia, confirming its role as the functional core of the intermunicipal transport network (see Figures 3, 4, and 7).

Betweenness centrality analysis further revealed that several secondary and tertiary roads—such as the Génova–Barragán–Armenia, Calarcá–Armenia, and Montenegro–El Caimo–La Tebaida corridors—play a disproportionately important structural role in regional connectivity despite their physical and operational limitations. This finding highlights a systemic vulnerability: The dependence of the transportation system on infrastructures that were not designed to support high traffic volumes or recurrent disturbance events (see Figure 5).

The eccentricity and eigenvector centrality metrics reinforce this interpretation by revealing a clear differentiation between highly integrated central zones and peripheral regions with a higher risk of isolation (see Figures 7 and 8). Taken together, the centrality analysis provides robust quantitative evidence of the structural bottlenecks of the Quindío road system and establishes a solid technical basis for prioritizing infrastructure interventions, strengthening the resilience of intermunicipal public transport, and improving territorial planning under disruption scenarios.

The additional comparison of centrality-based attack strategies provided further insight into the structural organization of the network. While degree centrality has traditionally been used to identify critical nodes, the results demonstrate that betweenness centrality is substantially more effective for detecting the elements whose removal produces the greatest loss of global connectivity. This finding indicates that the strategic role of a node within the transportation network depends not only on its number of connections but also on its function as a bridge linking different regions of the network.

In addition, the percolation analysis allowed the explicit evaluation of the structural resilience of the intermunicipal road network of Quindío under progressive failure scenarios. The initial comparison between random failures and targeted attacks confirmed that the network is considerably more vulnerable when strategically important nodes are removed than under random failures (see Table 1 and Figures 10–12). To further investigate this behavior, additional percolation experiments were performed using different node removal strategies based on degree, betweenness, and closeness centrality (Figure 13). The results demonstrate that attacks guided by betweenness centrality produce the fastest deterioration of the giant component, indicating that bridge nodes connecting different regions of the network play a more critical structural role than highly connected nodes alone. Degree-based attacks exhibit an intermediate response, whereas closeness-based attacks preserve global connectivity for a substantially longer period. These findings indicate that betweenness centrality is the most informative metric for identifying structurally critical elements in the Quindío road network and confirm that the vulnerability of the system is concentrated in a relatively small set of strategic nodes rather than being homogeneously distributed throughout the network.

Although the network structure provides alternative routes in the event of blockages along major corridors, the results show that several of these alternatives present operational limitations—such as unpaved and narrow roads—that make them unsuitable for regular intermunicipal public transport operations, particularly in terms of capacity, safety, and travel times. This behavior is characteristic of hierarchical networks with low functional redundancy, where localized failures—such as landslides, road closures, or extreme weather events—can trigger extensive disconnections and significant territorial isolation. From an operational and planning perspective, the percolation results highlight the need to prioritize the strengthening and redundancy of nodes and edges identified as critical, as well as to incorporate structural resilience criteria into infrastructure investment and intermunicipal transport management decisions.

Similarly, the results of the discrete event simulation applied to the Génova–Armenia intermunicipal route reveal the significant impact that both the structure of the road network and the local operational conditions have on the performance of the public transportation system. The simulation allowed the estimation of realistic travel times under different scenarios, showing that this route exhibits high sensitivity to variations in average speed and to partial interruptions of the corridor due to its mountainous layout and the limited availability of functional alternative routes.

Although the simulation is inspired by queueing theory, it should not be interpreted as a classical analytical queueing model. Instead, queueing concepts are used to represent operational events associated with vehicle movements, passengers boarding, and service times within a network-driven discrete event framework. This formulation provides sufficient flexibility to represent rural intermunicipal transportation while allowing future extensions incorporating demand-driven passenger arrival processes or more sophisticated stochastic arrival models.

The simulated scenarios confirmed that, under disruption events, increases in travel times are not linear but instead become amplified due to cumulative effects associated with intermediate stops, passengers' boarding and alighting times, and the geometric constraints of the road infrastructure. The comparison with reference travel times obtained from GPS navigation platforms showed reasonable agreement, supporting the validity of the proposed model. Overall, these results highlight the operational vulnerability of the Génova–Armenia route and emphasize the importance of incorporating dynamic and operational criteria, in addition to structural factors, in the planning and management of intermunicipal public transportation in the department.

The operational parameters adopted in the simulation were derived from field observations conducted on intermunicipal bus routes in the department of Quindío. In particular, passengers' boarding times reflect the operating conditions of rural transportation, where luggage and agricultural products frequently increase service times compared with typical urban systems. Consequently, the proposed model seeks to represent realistic regional operating conditions rather than relying exclusively on generic values reported in the literature.

Finally, this study demonstrates that the integrated use of tools based on complex network theory and discrete event simulation provides robust quantitative support for decision-making in road planning and intermunicipal public transport management. This approach goes beyond traditional descriptive analyses by providing objective criteria for identifying critical corridors, evaluating the structural resilience of the network, and anticipating the operational impacts of decisions such as road closures, temporary detours, or infrastructure interventions.

From a broader methodological perspective, this work contributes to reducing the gap between structural transportation network analysis and operational public transport simulations. Previous studies have generally focused either on the topological characterization of transportation networks or on stochastic simulations of transportation operations. By explicitly integrating both perspectives within a single computational framework, the proposed methodology enables the simultaneous evaluation of structural vulnerability, operational performance, and disruption management, providing a more comprehensive tool for transportation planning in geographically constrained regions.

In particular, the ability to combine centrality metrics, percolation analysis, and dynamic simulations offers transportation authorities and territorial planners an effective tool for prioritizing investments, designing contingency plans, and improving the efficiency of public transport services under conditions of climatic and operational uncertainty. In this sense, the systematic adoption of these methodologies can significantly contribute to a more resilient, efficient, and evidence-based management of regional transportation systems.

This integrated methodology is readily transferable to other intermunicipal transportation systems where infrastructural constraints, geographical complexity, and operational uncertainty play a decisive role in mobility planning and resilience assessment.

Use of AI tools declaration

The authors used an artificial intelligence tool (ChatGPT, OpenAI) to assist in improving the English language and clarity of the manuscript. All scientific content, methodology, and results were developed and verified by the authors.

Acknowledgments

The authors acknowledge the financial and academic support of the Universidad del Quindío in the development of this research. (Crossref code of financing: 100016837).

Conflict of interest

The authors declare there is no conflict of interest.

Author contributions

Conceptualization: Jorge Mario Garcia-Usuga and Monica Jhoana Mesa-Mazo. Methodology: Jorge Mario Garcia-Usuga and Monica Jhoana Mesa-Mazo. Software: Jorge Mario Garcia-Usuga. Validation: Jorge Mario Garcia-Usuga, Monica Jhoana Mesa-Mazo, and Jhoana P. Romero-Leiton. Formal analysis: Jorge Mario Garcia-Usuga and Jhoana P. Romero-Leiton. Investigation: Jorge Mario Garcia-Usuga, Monica Jhoana Mesa-Mazo, and Jhoana P. Romero-Leiton. Data curation: Jorge Mario Garcia-Usuga. Writing—original draft: Jorge Mario Garcia-Usuga. Writing—review and editing: Monica Jhoana Mesa-Mazo and Jhoana P. Romero-Leiton. Visualization: Jorge Mario Garcia-Usuga and Monica Jhoana Mesa-Mazo Supervision: Jorge Mario Garcia-Usuga and Monica Jhoana Mesa-Mazo. Project administration: Jorge Mario Garcia-Usuga and Monica Jhoana Mesa-Mazo. Funding acquisition: Jorge Mario Garcia-Usuga and Monica Jhoana Mesa-Mazo.

All authors have read and agreed to the published version of the manuscript.

References

1. INRIX Research, *2024 Global Traffic Scorecard*, Technical report, INRIX, Inc., Kirkland, WA, 2024 (Accessed: January 2025). Available from: https://inrix.com/scorecard/.

2. TomTom Traffic Index, *TomTom Traffic Index 2023: Global Traffic Congestion Rankings*, Technical report, TomTom International BV, 2024 (Accessed: January 2024). Available from: https://www.tomtom.com/.

3. BRT Data, Global BRT Data—Ridership Statistics, Online database, 2023 (Accessed: September 2024). Available from: https://brtdata.org/.

4. EMBARQ, On the Move: The Global Rise of Mass Transit, Smart Cities Dive, 2014. Available from: https://www.smartcitiesdive.com/ex/sustainablecitiescollective/move-global-rise-mass-transit/200656/.

5. UITP—International Association of Public Transport, *Global Economic Outlook 2024: Public Transport Trends and Statistics*, Technical report, UITP, Brussels, Belgium, 2024 (Accessed: September 2024). Available from: https://www.uitp.org/publications/global-economic-outlook-2024/.

6. D. C. Mestra Sierra, M. A. Rodriguez Peniche, D. M. Rodriguez Herrera, T. O. Boyano Fram, Land transport mobility in the urban-rural context of Colombia, *Saber Cienc. Libertad Germ.*, **17** (2024), 162–168. https://doi.org/10.18041/2382-3755/germinacion.2024v17.12233

7. L. A. Guzman, S. G. Cardona, J. L. Ochoa, Increased ridership and improved affordability: Transforming public transport subsidies in developing contexts, *Res. Transp. Econ.*, **108** (2024), 101492. https://doi.org/10.1016/j.retrec.2024.101492

8. M. Islam, G. Kabir, M. R. Anis, Evaluating enso-driven risks to strengthen transportation system resilience of canadian provinces, *Can. J. Civ. Eng.*, **52** (2025), 1630–1644. https://doi.org/10.1139/cjce-2025-0118

9. H. A. Moreno, M. C. Vélez Ortiz, J. D. Montoya, R. Rhenals Monterrosa, Rainfall and landslides in Antioquia: Analysis of their occurrence at interannual, intra-annual, and daily scales, *Rev. EIA*, **5** (2006), 59–69. Available from: https://dialnet.unirioja.es/servlet/articulo?codigo=5557900.

10. O. Bello, L. Ortiz, J. Samaniego, *Estimation of the Effects of Disasters in Latin America, 1972–2010*, CEPAL, Medio Ambiente y Desarrollo Series No. 157, LC/L.3899, United Nations, Santiago, Chile, 2014 (Accessed: January 2025). Available from: https://repositorio.cepal.org/server/api/core/bitstreams/f10005fd-faf1-4fe4-8edf-40d0cc33fd16/content.

11. S. Boccaletti, V. Latora, Y. Moreno, M. Chavez, D. U. Hwang, Complex networks: Structure and dynamics, *Phys. Rep.*, **424** (2006), 175–308. https://doi.org/10.1016/j.physrep.2005.10.009

12. E. Estrada, *The Structure of Complex Networks: Theory and Applications*, Oxford University Press, 2011. https://doi.org/10.1093/acprof:oso/9780199591756.001.0001

13. M. Newman, *Networks*, Oxford University Press, 2018. https://doi.org/10.1093/oso/9780198805090.001.0001

14. Z. Xu, S. S. Chopra, H. Lee, Resilient urban public transportation infrastructure: A comparison of five flow-weighted metro networks in terms of the resilience cycle framework, *IEEE Trans. Intell. Transp. Syst.*, **23** (2022), 12688–12699. https://doi.org/10.1109/tits.2021.3116667

15. C. Chen, S. Wang, J. Zhang, X. Gu, Modeling the vulnerability and resilience of interdependent transportation networks under multiple disruptions, *J. Infrastruct. Syst.*, **29** (2023), 04022043. https://doi.org/10.1061/jitse4.iseng-2185

16. J. Tang, L. Xu, C. Luo, T. S. A. Ng, Multi-disruption resilience assessment of rail transit systems with optimized commuter flows, *Reliab. Eng. Syst. Saf.*, **214** (2021), 107715. https://doi.org/10.1016/j.ress.2021.107715

17. N. Yadav, S. Chatterjee, A. R. Ganguly, Resilience of urban transport network-of-networks under intense flood hazards exacerbated by targeted attacks, *Sci. Rep.*, **10** (2020), 10350. https://doi.org/10.1038/s41598-020-66049-y

18. R. W. Hall, Transportation queueing, in *Handbook of Transportation Science*, 2003, 113–153. https://doi.org/10.1007/0-306-48058-1_5

19. N. Gautam, *Analysis of Queues: Methods and Applications*, CRC Press, 2012. https://doi.org/10.1201/b11858

20. B. X. Dong, M. Shan, B. G. Hwang, Simulation of transportation infrastructures resilience: A comprehensive review, *Environ. Sci. Pollut. Res.*, **29** (2022), 12965–12983. https://doi.org/10.1007/s11356-021-18033-w

21. M. Neagoe, H. H. Hvolby, M. S. Taskhiri, P. Turner, Using discrete-event simulation to compare congestion management initiatives at a port terminal, *Simul. Model. Pract. Theory*, **112** (2021), 102362. https://doi.org/10.1016/j.simpat.2021.102362

22. Z. Lyu, D. Pons, Y. Zhang, Z. Ji, Freight operations modelling for urban delivery and pickup with flexible routing: Cluster transport modelling incorporating discrete-event simulation and GIS, *Infrastructures*, **6** (2021), 180. https://doi.org/10.3390/infrastructures6120180

23. O. A. Sediek, S. El-Tawil, J. McCormick, Modeling interdependencies between the building portfolio, transportation network, and healthcare system in community resilience, *Nat. Hazards Rev.*, **23** (2022), 04021060. https://doi.org/10.1061/(asce)nh.1527-6996.0000538

24. S. Dudin, A. Dudin, R. Manzo, L. Rarità, Analysis of semi-open queueing network with correlated arrival process and multi-server nodes, *Oper. Res. Forum*, **5** (2024), 99. https://doi.org/10.1007/s43069-024-00383-z

25. A. Dudin, S. Dudin, R. Manzo, L. Rarità, Queueing system with batch arrival of heterogeneous orders, flexible limited processor sharing and dynamical change of priorities, *AIMS Math.*, **9** (2024), 12144–12169. https://doi.org/10.3934/math.2024593

26. A. Dudin, S. Dudin, R. Manzo, L. Rarità, Analysis of multi-server priority queueing system with hysteresis strategy of server reservation and retrials, *Mathematics*, **10** (2022), 3747. https://doi.org/10.3390/math10203747

27. G. Boeing, OSMnx: New methods for acquiring, constructing, analyzing, and visualizing complex street networks, *Comput. Environ. Urban Syst.*, **65** (2017), 126–139. https://doi.org/10.1016/j.compenvurbsys.2017.05.004

28. G. Boeing, Urban street network analysis in a computational notebook, *REGION*, **6** (2020), 39–51. https://doi.org/10.18335/region.v6i3.278

29. P. Crucitti, V. Latora, S. Porta, Centrality measures in spatial networks of urban streets, *Phys. Rev. E*, **73** (2006), 036125. https://doi.org/10.1103/physreve.73.036125

30. W. Liu, X. Li, T. Liu, B. Liu, Approximating betweenness centrality to identify key nodes in a weighted urban complex transportation network, *J. Adv. Transp.*, **2019** (2019), 9024745. https://doi.org/10.1155/2019/9024745

31. Departamento Administrativo Nacional de Estadística (DANE), Censo Nacional de Población y Vivienda (CNPV) 2018: Presentación Quindío—Armenia, 2019 (Accessed: January 30, 2026). Available from: https://www.dane.gov.co/files/censo2018/informacion-tecnica/presentaciones-territorio/190731-CNPV-presentacion-Quindio-Armenia.pdf.

32. OpenStreetMap contributors, OpenStreetMap, 2024 (Accessed: January 30, 2026). Available from: https://www.openstreetmap.org/.

33. R. Diestel, *Graph Theory*, 5th (ed), Springer, Berlin, 2017. https://doi.org/10.1007/978-3-662-53622-3

34. S. H. Strogatz, Exploring complex networks, *Nature*, **410** (2001), 268–276. https://doi.org/10.1038/35065725

35. L. Fraccascia, I. Giannoccaro, V. Albino, Resilience of complex systems: State of the art and directions for future research, *Complexity*, **2018** (2018), 3421529. https://doi.org/10.1155/2018/3421529

36. L. D. F. Costa, Reinforcing the resilience of complex networks, *Phys. Rev. E*, **69** (2004), 066127. https://doi.org/10.1103/physreve.69.066127

37. G. Paul, S. Sreenivasan, H. E. Stanley, Resilience of complex networks to random breakdown, *Phys. Rev. E*, **72** (2005), 056130. https://doi.org/10.1103/physreve.72.056130

38. J. Gao, B. Barzel, A. L. Barabási, Universal resilience patterns in complex networks, *Nature*, **530** (2016), 307–312. https://doi.org/10.1038/nature16948

39. SimPy Community, SimPy Documentation (Accessed: January 7, 2026). Available from: https://simpy.readthedocs.io/.

40. J. Zhang, Y. Luo, Degree centrality, betweenness centrality, and closeness centrality in social network, in *2017 2nd International Conference on Modelling, Simulation and Applied Mathematics (MSAM2017)*, Bankog, Thailand, 2017, 300–303. https://doi.org/10.2991/msam-17.2017.68

41. E. Cohen, D. Delling, T. Pajor, R. F. Werneck, Computing classic closeness centrality, at scale, in *COSN '14: Proceedings of the second ACM conference on Online social networks*, New York, NY, USA, 2014, 37–50. https://doi.org/10.1145/2660460.2660465

42. A. Cuzzocrea, A. Papadimitriou, D. Katsaros, Y. Manolopoulos, Edge betweenness centrality: A novel algorithm for QoS-based topology control over wireless sensor networks, *J. Netw. Comput. Appl.*, **35** (2012), 1210–1217. https://doi.org/10.1016/j.jnca.2011.06.001

43. A. Kazerani, S. Winter, Can betweenness centrality explain traffic flow, in *Proceedings of the 12th AGILE International Conference*, Springer, 2009.

44. M. Newman, *Networks: An Introduction*, Oxford University Press, 2010. https://doi.org/10.1093/acprof:oso/9780199206650.001.0001

45. M. Krnc, J. S. Sereni, R. Škrekovski, Z. B. Yilma, Eccentricity of networks with structural constraints, *Discuss. Math. Graph Theory*, **40** (2020), 1141–1162. https://doi.org/10.7151/dmgt.2180

46. Y. Zhang, *New Frontiers in Graph Theory*, Intech, 2012. https://doi.org/10.5772/1965

47. P. Bonacich, Some unique properties of eigenvector centrality, *Soc. Networks*, **29** (2007), 555–564. https://doi.org/10.1016/j.socnet.2007.04.002

48. B. Ruhnau, Eigenvector-centrality—A node-centrality? *Soc. Networks*, **22** (2000), 357–365. https://doi.org/10.1016/s0378-8733(00)00031-9

49. L. Solá, M. Romance, R. Criado, J. Flores, A. García del Amo, S. Boccaletti, Eigenvector centrality of nodes in multiplex networks, *Chaos*, **23** (2013), 033131. https://doi.org/10.1063/1.4818544

50. S. Porta, P. Crucitti, V. Latora, The network analysis of urban streets: A dual approach, *Physica A*, **369** (2006), 853–866. https://doi.org/10.1016/j.physa.2005.12.063

51. P. Crucitti, V. Latora, S. Porta, Centrality in networks of urban streets, *Chaos*, **16** (2006), 015113. https://doi.org/10.1063/1.2150162

52. E. López, R. Parshani, R. Cohen, S. Carmi, S. Havlin, Limited path percolation in complex networks, *Phys. Rev. Lett.*, **99** (2007), 188701. https://doi.org/10.1103/physrevlett.99.188701

53. M. A. Serrano, M. Boguñá, Clustering in complex networks. II. Percolation properties, *Phys. Rev. E*, **74** (2006), 056115. https://doi.org/10.1103/physreve.74.056115

54. R. Cohen, S. Havlin, *Percolation in Complex Networks*, Springer, New York, NY, 2021, 419–431. https://doi.org/10.1007/978-1-0716-1457-0_383

55. A. Allard, L. Hébert-Dufresne, Percolation and the effective structure of complex networks, *Phys. Rev. X*, **9** (2019), 011023. https://doi.org/10.1103/physrevx.9.011023

56. Y. Y. Liu, E. Csóka, H. Zhou, M. Pósfai, Core percolation on complex networks, *Phys. Rev. Lett.*, **109** (2012), 205703. https://doi.org/10.1103/physrevlett.109.205703

57. M. Li, R. R. Liu, L. Lü, M. B. Hu, S. Xu, Y. C. Zhang, Percolation on complex networks: Theory and application, *Phys. Rep.*, **907** (2021), 1–68. https://doi.org/10.1016/j.physrep.2020.12.003